Five-year correlation of the Sun shadow in cosmic rays observed by ARGO-YBJ with the interplanetary magnetic field variability

F.R. Zhu [*][†]

School of Physical Science and Technology, Southwest Jiaotong University, Chengdu 610031, China
E-mail: zhufr@ihep.ac.cn

D. Ruffolo

Department of Physics, Faculty of Science, Mahidol University, Bangkok 10400, Thailand
E-mail: ruffolo.physics@gmail.com

Z. Cao

Key Laboratory of Particle Astrophysics, Institute of High Energy Physics, CAS, 100049, Beijing, China
E-mail: caozh@ihep.ac.cn

H.Y. Jia

School of Physical Science and Technology, Southwest Jiaotong University,Chengdu 610031, China
E-mail: jiahy@ihep.ac.cn

The shadow that the Sun casts on high energy cosmic rays is affected by the solar, interplanetary, and terrestrial magnetic fields and has been shown to vary according to the solar rotation and activity cycle. Using the data of the ARGO-YBJ experiment, a large-area air shower detector located at high mountain altitude (4300 m a.s.l., in Tibet, China), the deficit of ~ 5 TeV cosmic rays due to the Sun shadowing effect has been monitored on a three-month basis from November 2007 to February 2013, a time interval that includes a period of very low solar activity, followed by an activity increase towards the sunspot maximum. We found that the Sun shadow deficit started to decrease significantly in early 2010, about one year before the sunspot number had a fast increase, in early 2011. We observed indeed a significant anti-correlation between the Sun shadow deficit and the Interplanetary Magnetic Field (IMF) variability. This variability became more evident from early 2010, when the IMF showed frequent fluctuations and reversals, that could account for the observed decreased deficit of the shadow.

The 34th International Cosmic Ray Conference,
30 July- 6 August, 2015
The Hague, The Netherlands

---

[*]Speaker.

[†]on behalf of the ARGO-YBJ collaboration

1. Introduction

Cosmic rays of TeV-range energies from outside the solar system, mainly hydrogen and helium nuclei [1], arrive nearly isotropically at the Earth and can be recorded by detectors on the ground, such as the resistive plate chamber array of the ARGO-YBJ experiment [2] located in Tibet, China at 30.11°N, 90.53°E, 4300 m above sea level. The arrival direction distribution shows deficits corresponding to the locations of the Sun and Moon [3]. The solar, interplanetary, and terrestrial magnetic fields deflect the particle paths and shift the shadow of the Sun from its actual location, as first reported by the Tibet AS experiment [4]. In other words, the measured deflection of cosmic rays is a cumulative effect of magnetic fields along the whole path from the Sun to the Earth. This experiment also observed the effect of the interplanetary magnetic field (IMF) [5] and a solar cycle variation [6], and evaluated the effects of two coronal magnetic field models [7]: the potential field source surface (PFSS) [8, 9] and current sheet source surface (CSSS) models [10, 11].

The ARGO-YBJ experiment first used the Sun shadow displacement in the south-north direction to measure the intensity of the magnetic field that is transported by the solar wind from the Sun to the Earth, during the recent period of minimum solar activity [12]. This experiment also found that the deficit of cosmic ray flux in the shadow is reduced with increasing solar activity [13, 14, 15]. To understand the shadow effect, it is useful to imagine trajectories of antiparticles traveling backward from Earth to intersect the Sun's surface, which are equivalent to the forward trajectories that are blocked by the Sun, causing the shadow. One possible explanation of weaker Sun shadow with increasing solar activity is that if the solar coronal magnetic fields are very irregularly distributed, the cosmic ray deflections could be so randomized that backwards trajectories over a wider range of angles can intersect the Sun. In this paper, we consider another mechanism: variation and frequent reversals of the IMF during each three-month observation period causes a superposition of Sun shadows with different shifts and leads to an observed shadow that is wider and weaker. We demonstrate that the dependence of the Sun shadow deficit with time as observed by ARGO-YBJ from December, 2007 to February, 2013 is well associated with variability of the IMF.

2. The ARGO-YBJ experiment

The ARGO-YBJ experiment, located at the Yangbajing Cosmic Ray Observatory (Tibet, China, 4300m a.s.l.), consists of a single layer of resistive plate chambers (RPCs) distributed on a surface of 78×74 m^2. This full coverage area is divided into 10×13 clusters made of 12 RPCs ($\sim 2.85 \times 1.23$ m^2) each. Each chamber is read by 80 external strips of 6.75×61.80 cm^2 (the spatial pixels), logically organized in 10 independent pads of 55.6×61.8 cm^2 which represent the time pixels of the detector. Around this array, a guard ring made of 23 clusters with a coverage of 25% is designed to improve the event reconstruction. The readout of 18360 pads and 146880 strips is the experimental output of the detector.

ARGO-YBJ operated in two independent data acquisition modes: the shower mode and the scaler mode [16]. In shower mode, all showers with a number of hits $N_{hits} \geq 20$ in the central carpet in a time window of 420 ns generate a trigger, and the trigger rate was about 3.5 kHz. The events collected in shower mode contain both digital and analog information on the shower particles [17].

In this analysis we refer to the digital data recorded in shower mode. The primary arrival direction is determined by fitting the arrival times of the shower front particles. The angular resolution for cosmic ray induced showers has been checked using the Moon shadow, observed by ARGO-YBJ with a statistical significance of ∼10 standard deviations for $N_{hits} \geq 100$ each month. The shape of the shadow provided a measurement of the detector PSF, which has been found to agree with expectations [3].

The pad multiplicity is used as an estimator of the primary cosmic ray energy via a relationship inferred from Monte Carlo simulations. The reliability of the energy scale has been tested with the Moon shadow. Due to the geomagnetic field, cosmic rays are deflected according to their energy and the Moon shadow is shifted with respect to the Moon position by an amount depending on the primary energy. The westward shift of the shadow has been measured for different N_{hits} intervals and compared with simulations. We found that the total absolute energy scale error is less than 13% in the proton energy range ∼1-30 TeV, including the uncertainties in the cosmic ray elemental composition and the hadronic interaction model [3].

3. Data analysis

In this work cosmic ray data recorded from 2007 Nov. 5 through 2013 Feb. 14 have been analyzed. Selection criteria are: (a) number of fired pads on the carpet greater than 100, (b) reconstructed zenith angle less than 50°, (c) reconstructed shower core positions within a distance of 150 m from the center of the array, (d) χ^2 of the reconstructed shower temporal front less than 200 ns^2. Finally, events within a cone of 6° with respect to the Sun and the Moon position have been analyzed separately. A total of 1.873×10^8 events for the Sun shadow and 1.887×10^8 for the Moon shadow survived all these cuts. To estimate the statistical significance of the Sun shadow observation, we analyzed the maps with the so-called equizenith angle method as described previously for the Moon shadow [3]. According to the absolute energy scale calibration from the Moon shadow analysis, the median energy of the selected data is about 5 TeV. The estimated angular resolution is better than 1°[3].

3.1 Sun shadow analysis

The observed Sun shadow is a superposition of the effects of the solar, interplanetary, and terrestrial magnetic fields. Temporal changes in the Sun shadow can be clearly observed in Figure 1 where 20 maps of the Sun region are shown. The ARGO-YBJ data have been divided according to astronomical seasons in the Northern Hemisphere and separately analyzed. The smoothing radius is 1.2° and the pixels are 0.1° × 0.1° large. The color represents the fractional deficit for each pixel. The contours indicate statistical significance, with a 1σ difference between neighbouring contours. The statistical significance of the innermost dark blue contour is 5σ smaller than the greatest deficit statistical significance in the map, and 5σ greater than its neighbouring dark blue contour, and so on. The significance for each pixel is calculated using equation(5) of [18]. The first and fourth columns show the Sun shadow observed during Winter and Autumn when the Sun observation time below 50° zenith angle is reduced with respect to Spring and Summer (second and third columns). Therefore, the statistical significance is weaker in Winter and Autumn, though the fractional deficit is comparable. As shown in [15], with increasing solar activity the shadows are

3
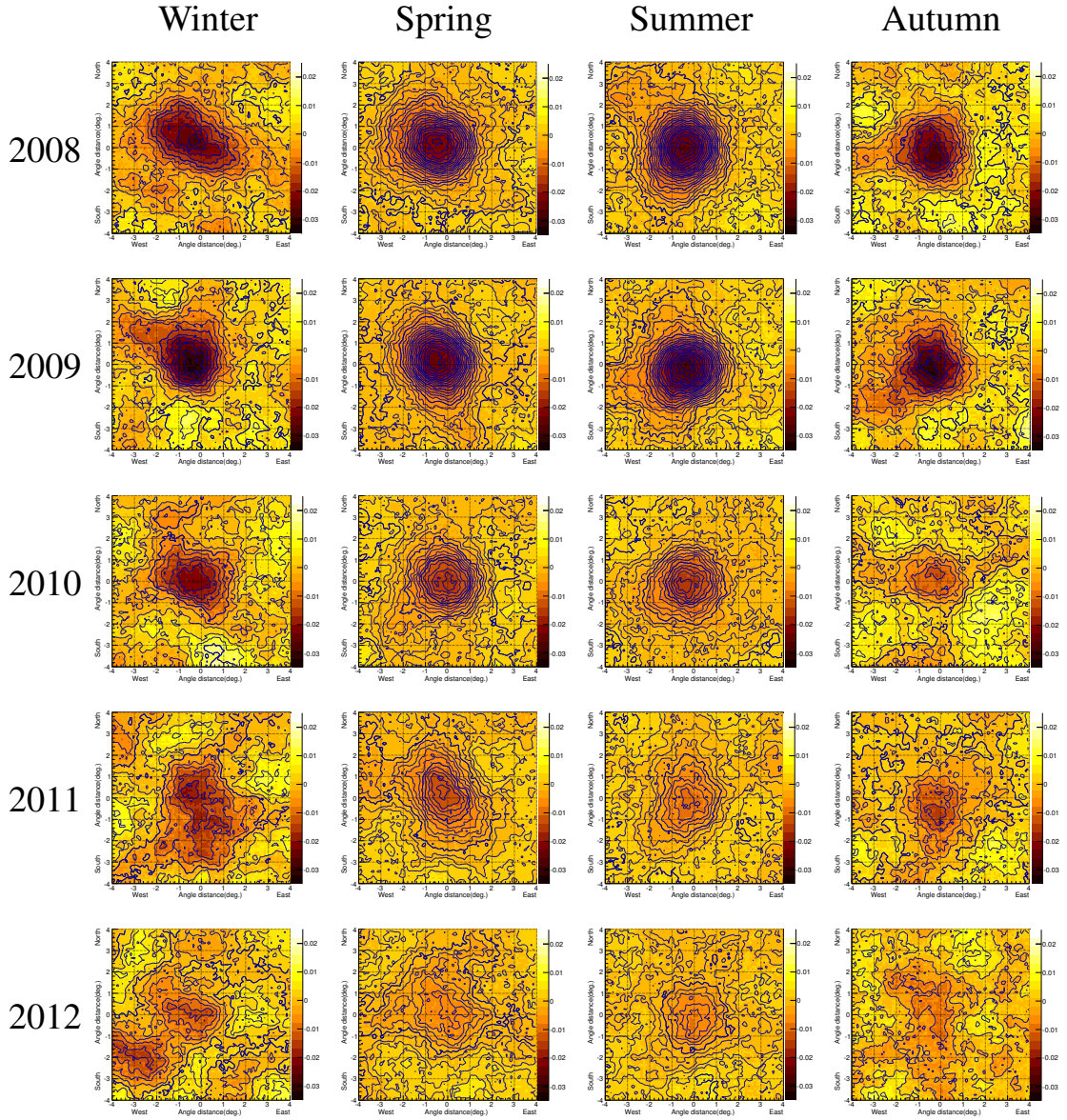
Figure 1: Seasonal variation in the Sun shadow observed by the ARGO-YBJ experiment in cosmic rays at median energy 5 TeV. The observation period for each map is one astronomical season in the Northern Hemisphere. The smoothing radius is $1.2°$ and the pixels are $0.1° \times 0.1°$. Each map shows the fractional change in the cosmic ray flux (color scale) and the statistical significance of the change (contours). Each contour represents an integral value of the significance (in units of the standard deviation), with darker contours every 5 units. Maps for the Spring and Summer seasons show stronger significance because the Sun was higher in the sky at the ARGO-YBJ site in Tibet. The fractional change suddenly weakened in Winter 2010, in association with a sudden increase in IMF variability, whereas the sunspot number and some other generic indicators of solar activity started to increase rapidly only in Spring 2011.

increasingly washed out. It is very interesting that there is a clear sudden change in the Sun shadow in Winter 2010 compared with Autumn 2009, which occurred together with enhanced variability of the IMF, as will be explained shortly.

4
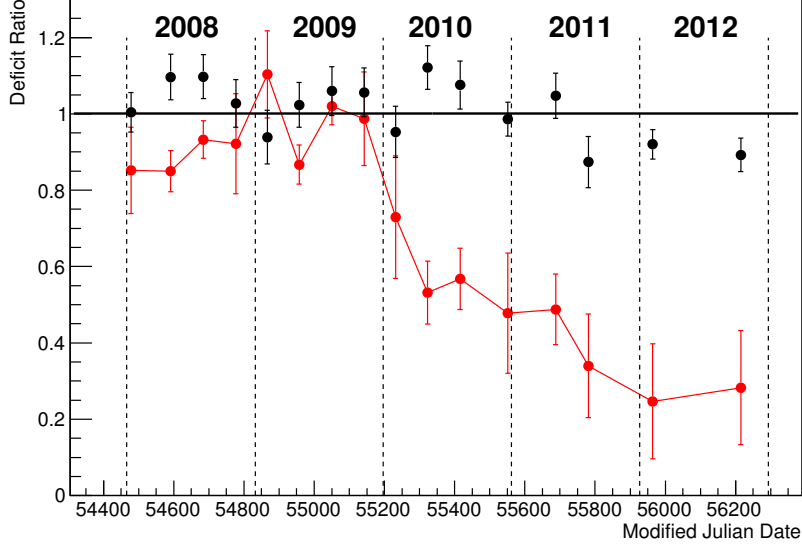
Figure 2: Deficit ratio of the observed to expected numbe of events as a function of the observation season for the Sun shadow (red points) and Moon shadow (black points). The error bars show the statistical error. The Moon shadow remains roughly constant while the Sun shadow weakens during times of greater solar activity.

3.2 Deficit ratio of Sun shadow and Moon shadow

To obtain Sun and Moon shadow maps with sufficient statistical significance, Sun and Moon shadow data from some seasons were merged, resulting in 16 time periods from November 2007 through February 2013. Specifically, we merged late 2007 with Winter 2008, Autumn 2010 with Winter 2011, Autumn 2011 with Winter and Spring 2012, and the rest of 2012 with early 2013.

To quantify the weakening of the Sun shadow, which may be due to spreading over a wider angular range, we measure a deficit ratio between the observed and expected (geometric) number of events in the Sun shadow and Moon shadow. Assuming that the shadow has a binormal distribution, the observed deficit in events, $N_{def}(< R)$, within an angular distance R from the Sun's center is given by

$$N_{def}(< R) = \left[1 - e^{-\frac{R^2}{2\sigma^2}}\right] \cdot N_{Sun} \tag{3.1}$$

where N_{Sun} is the total number of events intercepted by the Sun and σ is the Gaussian width of the shadow. However, in this work N_{Sun} is estimated by fitting Eq. (3.1) to the experimental points for fixed $\sigma = 1.2°$, so it instead serves to measure the central depth of the shadow. The expected (geometric) deficit events are simply counted from the background within the solar disc. The deficit ratios of the Sun shadow for the 16 time intervals are shown by red points in Figure 2. During the years 2008 and 2009, the deficit ratio was about 1, but starting in early 2010 it decreased rapidly and then more gradually to 0.2, while the deficit ratio of the Moon shadow was stable near 1 as shown in Figure 2, which is consistent with good detector performance.
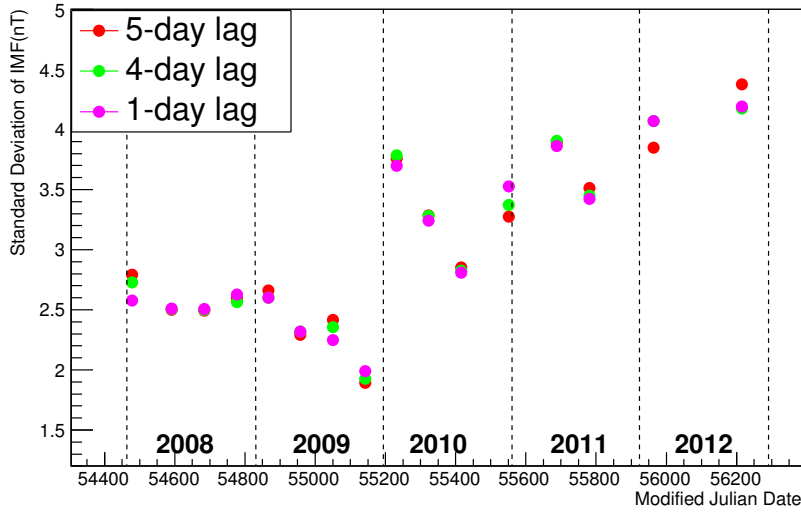
Figure 3: Root mean squared variation of the vector IMF during each time period of Sun shadow. This rose sharply in early 2010, as the Sun shadow deficit ratio sharply decreased, suggesting a causal relationship. Different colors indicate different lags

3.3 Temporal variability of Interplanetary Magnetic Field

The sunspot number and the solar radio flux density are key indicators of solar activity. The larger the number of sunspots , the more active the Sun. The solar radio flux density at 10.7 cm (F10.7cm) is a measure of the noise level generated by the Sun. This radio flux, which originates from atmospheric layers high in the Sun's chromosphere and low in its corona, changes gradually from day to day, in response to the number of sunspot groups on the disk. As shown in [15], solar activity was in its quiet phase during 2008 and 2009, increased gradually in 2010, and then rapidly increased in early 2011.

The IMF originates from the solar corona. When the Sun rotates, magnetic field lines are largely frozen into the solar wind and stretched out from the Sun along spiral patterns [19]. As the solar wind velocity increases the direction of the IMF becomes more radial, while if the solar wind is slow the direction of the IMF becomes more azimuthal. Abnormally strong IMF fluctuations can severely disturb the geomagnetic environment. We use IMF data measured by the ACE/MAG instrument at the L1 point. Figure 3 shows the temporal standard deviation of the IMF for the 16 time intervals over which the Sun shadow deficit ratio was determined, i.e., the square root of the sum of time-averaged variances in the x-, y-, and z-components of the IMF, weighted by the number of events observed with the ARGO-YBJ experiment before a certain lag time. Note that cosmic ray trajectories from the Sun travel through the IMF between the Sun and Earth, and the solar wind drags the IMF over that distance in ∼4 days, so the cosmic rays arriving at Earth at a given time are responding to the IMF at Earth at that time, and also to the IMF near the Sun, which will arrive at Earth with a lag of 4 days, as well as the IMF in between. Thus in Figure 3, we plot the standard deviation of the IMF weighted according to the cosmic ray flux, where the IMF is measured after a
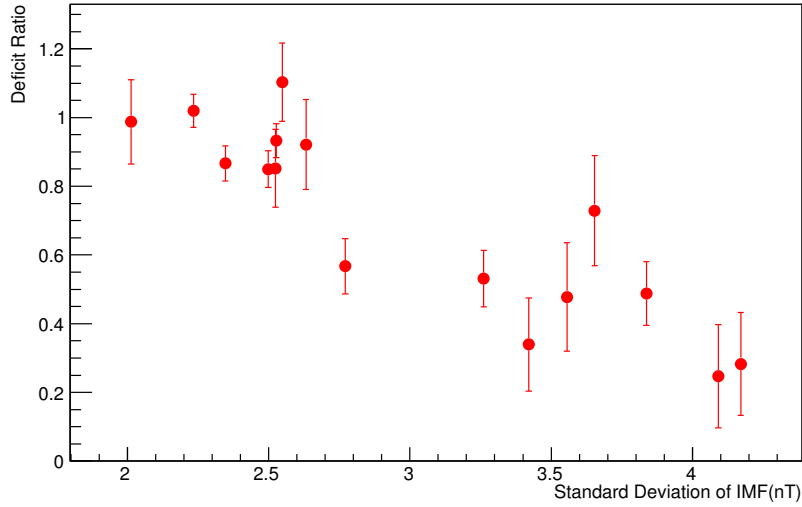
Figure 4: Deficit ratio observed by the ARGO-YBJ experiment vs. IMF variability. The horizontal axis gives the standard deviation of the IMF for each time period.

lag time of 1, 4, or 5 days. The variation of IMF is smaller in 2008 and 2009, and changed suddenly in early 2010, but there is no clear dependence on the lag time.

3.4 Correlation between variability of Interplanetary Magnetic Field and deficit ratio observed by the ARGO-YBJ experiment

The IMF can deflect the cosmic rays and shift the shadow from the Sun's location as found during the solar quiet phase [12]. A varying IMF implies a time-varying shift, which when integrated over an observation period of at least 3 months implies a spread in the Sun shadow. This leads to a lower deficit ratio as defined here, and their significant linear anti-correlation is shown in Figure 4. Two statistics, the Pearson correlation coefficient and discrete correlation function (DCF, [20]), are used to estimate the correlation between the deficit ratio observed by the ARGO-YBJ experiment and the variability of the IMF. Here Pearson's correlation coefficient between the deficit ratio of cosmic rays and the variability of the IMF is $-88 \pm 13\%$. The DCF is used to quantify the degree of correlation and the phase differences (lags) and it is $-93 \pm 24\%$ for the time lag of zero. Thus the IMF variability has a better association with changes in the Sun shadow deficit ratio observed by ARGO-YBJ than generic indicators of solar activity like the sunspot number and F10.7cm flux.

4. Summary

Using the data obtained with the ARGO-YBJ experiment from November 2007 to February 2013, for the first time we monitored the Sun shadow on a quarterly basis with high statistical significance. We confirmed that the shadow of the Sun was more washed out as solar activity increased towards the maximum of the Solar Cycle 24. A detailed study of the correlation between variability of the IMF and the cosmic ray deficit is reported in this paper. The upcoming Large High-Altitude

Air Shower Observatory (LHAASO) experiment [21] should obtain sufficient statistics to observe the Sun shadow on a daily basis to monitor IMF variation and help forecast space weather.

Acknowledgments

References

[1] H. S. Ahn, et al., 2010, ApJ, 714, L89.

[2] G. Aielli, et al.(ARGO-YBJ Collaboration), 2006, Nucl. Instrum. Methods Phys. Res. A, 562, 92.

[3] B. Bartoli, et al.(ARGO-YBJ Collaboration), 2011, Phys. Rev. D, 84, 022003.

[4] M. Amenomori, et al., 1993a, Phys. Rev. D, 47, 2675.

[5] M. Amenomori, et al., 1993b, ApJ, 415, L147.

[6] M. Amenomori, et al., 1996, ApJ, 464, 954.

[7] M. Amenomori, et al., 2013, Phys. Rev. Lett., 111, 011101.

[8] K. H. Schatten, J. M. Wilcox, and N. F. Ness, 1969, Sol. Phys., 6, 442.

[9] K. Hakamada, 1995, Sol. Phys., 159, 89.

[10] T. J. Bogdan, B. C. Low, 1986, Astrophys. J., 306, 271.

[11] X. P. Zhao, J. T. Hoeksema, 1995, J. Geophys. Res., 100, 19.

[12] G. Aielli, et al.(ARGO-YBJ Collaboration), 2011, ApJ, 729, 113.

[13] F. R. Zhu, et al. (ARGO-YBJ Collaboration), 2009, ICRC.

[14] F. R. Zhu, et al. (ARGO-YBJ Collaboration), 2011, ICRC, 11, 158.

[15] F. R. Zhu, et al. (ARGO-YBJ Collaboration), 2013, ICRC.

[16] G. Aielli, et al.(ARGO-YBJ Collaboration), 2008, Astropart. Phys., 30, 85.

[17] G. Aielli, et al.(ARGO-YBJ Collaboration), 2015, Astropart. Phys., 67, 47.

[18] T. P. Li, Y. Q. Ma, 1983, ApJ, 272, 317.

[19] E. N. Parker, 1958, ApJ, 128, 664.

[20] R. R. Edelson, J. H. Krolik, 1988, ApJ, 333, 646.

[21] Z. Cao, et al. (LHAASO Collaboration), 2010, Chin. Phys. C, 34, 249.